



## A BRIEF REVIEW ON CORROSION INHIBITION STUDY OF ORGANIC LIGAND: ELECTROCHEMICAL, MORPHOLOGY, AND ISOTHERM STUDIES

(Ulasan Ringkas Terhadap Kajian Perencatan Kakisan Ligan oleh Ligan Organik: Kajian Elektrokimia, Morfologi dan Isotherma)

Nur Nadia Dzulkifli<sup>1,3\*</sup>, Nur Zalin Khaleda Razali<sup>3</sup>, Norsanida Iswa Sahani<sup>3</sup>,  
Sheikh Ahmad Izaddin Sheikh Mohd Ghazali<sup>1,3</sup>, Dzeelfa Zainal Abidin<sup>2</sup>, Asiah Abdullah<sup>1,3</sup>, Nurazira Mohd Nor<sup>1,3</sup>

<sup>1</sup>*Material, Inorganic, and Oleochemistry (MaterInOleo) Research Group, Faculty of Applied Sciences*

<sup>2</sup>*Academy of Language Studies*

<sup>3</sup>*School of Chemistry and Environment, Faculty of Applied Sciences*

*Universiti Teknologi MARA Cawangan Negeri Sembilan, Kampus Kuala Pilah, Pekan Parit Tinggi,  
72000 Kuala Pilah, Negeri Sembilan, Malaysia*

*\*Corresponding author: nurnadia@uitm.edu.my*

Received: 10 February 2022; Accepted: 2 April 2022; Published: 25 August 2022

### Abstract

Over the past decade, the corrosion inhibition of organic ligands has been extensively studied in numerous experiments in acid media. The number of published papers related to corrosion inhibition studies of organic ligands has been rising exponentially. The organic ligands have high inhibitive properties due to their capability to adsorb on the surface of metal by forming a protective layer. Having lone pair electrons (S, N, O) and multiple bonds ( $\pi$  bonds) allow them to adsorb on the surface of metals efficiently. However, there is very limited and less comprehensive information on the characterization of corrosion inhibition performance of organic ligands on the surface of metals. Therefore, this review paper provides a comprehensive review on the corrosion inhibition performance through various characterization methods, which are the electrochemical method [Electrochemical Impedance Spectroscopy (EIS), Polarization], Scanning Electron Microscope (SEM) with Energy Dispersive X-ray (EDX), and Langmuir Isotherm, which are thoroughly discussed herein.

**Keywords:** electrochemical impedance spectroscopy, polarization, scanning electron microscope with energy dispersive X-ray; Langmuir isotherm

### Abstrak

Sepanjang dekad yang lalu, perencatan kakisan ligan organik di dalam media berasid telah diuji di dalam eksperimen secara meluas dalam banyak eksperimen dalam media asid. Bilangan makalah yang diterbitkan berkaitan dengan kajian perencatan kakisan ligan organik telah meningkat secara eksponen. Ligan organik mempunyai sifat perencat yang tinggi kerana keupayaannya untuk menjerap pada permukaan logam dengan membentuk lapisan pelindung. Mempunyai pasangan elektron tunggal (S, N, O) dan ikatan berganda (ikatan  $\pi$ ) membolehkan ligan organik menjerap pada permukaan logam dengan berkesan. Walau bagaimanapun, terdapat maklumat yang sangat terhad dan kurang komprehensif mengenai pencirian prestasi perencatan kakisan ligan organik

pada permukaan logam. Oleh itu, kertas kajian ini menyediakan ulasan kajian secara menyeluruh tentang pencirian prestasi perencatan kakisan melalui pelbagai kaedah pencirian seperti kaedah elektrokimia [Spektroskopi Impedan Elektrokimia (EIS), Polarisasi], Mikroskop Elektron Pengimbas (SEM) dengan Sinar-X Serakan Tenaga (EDX), dan Isoterma Langmuir dan telah dibincangkan dengan teliti di sini.

**Kata kunci:** spektroskopi impedan elektrokimia, polarisasi, mikroskop elektron pengimbas dengan sinar-X serakan tenaga, isoterma Langmuir

### Introduction

Corrosion is the term used for the natural oxidation of metal. Corrosion is also prescribed as the electrochemical corrosion or deterioration of metals and alloys in the presence of an environment [1-2]. When metals and alloys are unprotected in an acidic environment, they corrode rapidly. When metals come into contact with inorganic acids, pits and cracks formation on the surface causes machinery and equipment to fail [3-4]. Organic and inorganic compounds are the two major classes of corrosion inhibitors. Inorganic corrosion inhibitors are legislation restricted due to their potential for toxicity and pollution, while organic inhibitors are the most common means of preventing metal corrosion in harsh environments [5-6]. The organic inhibitor, when introduced in small amounts to the environment where a metal would corrode, results in lessened oxidization of the metal [7-9]. By adsorbing on the metal surface and generating an obstacle that inhibits the metal active sites, the organic inhibitor improves mild steel's resistance to corrosive media [10]. Organic ligands having  $\pi$  bonds, C=N, and lone electron pairs (S, O, N) would produce high inhibitive characteristics because they can enhance effective adsorption by covalent bonding with metal atoms' unoccupied *d*-orbitals [11-13]. Khaled et al. proclaimed that the S and N atoms have been shown to have the capability to form stable complexes that are closely arranged in the coordination sphere of metal ions [14]. Inhibitor molecules adsorb on metal surfaces, forming thin films that prevents corrosion by 'insulating' the metal from the corrosive electrolyte and altering the processes as well as the kinetics of corrosion reactions [15]. The organic corrosion inhibitor can be

adsorbed on the metallic substrate through physical or chemical adsorption [16]. Multiple electrochemical and physical characterization techniques were used to deduce the nature of adsorption and evaluate the inhibitor's corrosion inhibition efficacy.

This review presents the electrochemical techniques, Electrochemical Impedance Spectroscopy (EIS) and Polarization, which have been used to evaluate the efficacy of organic compounds as corrosion inhibitors on the surface of metal. Besides, the adsorption behavior of the inhibitors was also thoroughly reviewed through EDX and isotherm characterization.

### Corrosion Inhibition Performance Studies

#### *Electrochemical impedance spectroscopy*

EIS is a common method for exploring organic-coated metals because it is a quick and easy approach to figure out the protective characteristics of organic inhibitors on metal surfaces [17]. Besides, Nikooa et al., proclaimed that EIS is a valuable tool for learning more about the corrosion inhibition characteristic of organic inhibitors and their mechanism of protection [18]. Corrosion inhibitors, 2-pyridinecarboxaldehyde thiosemicarbazone (2-PCT), 4-pyridinecarboxaldehyde thiosemicarbazone (4-PCT) [19], 4-(*N,N*-dimethylamino)benzaldehyde thiosemicarbazone (DMABT) [28] and {[ (Benzylsulfanyl) carbonothioyl] amino} acetic acid (BDTC), {[ (Propylsulfanyl) carbonothioyl] amino} acetic acid (PDTC) [18] structures, as shown in Figure 1, are examples that are used for the discussion.

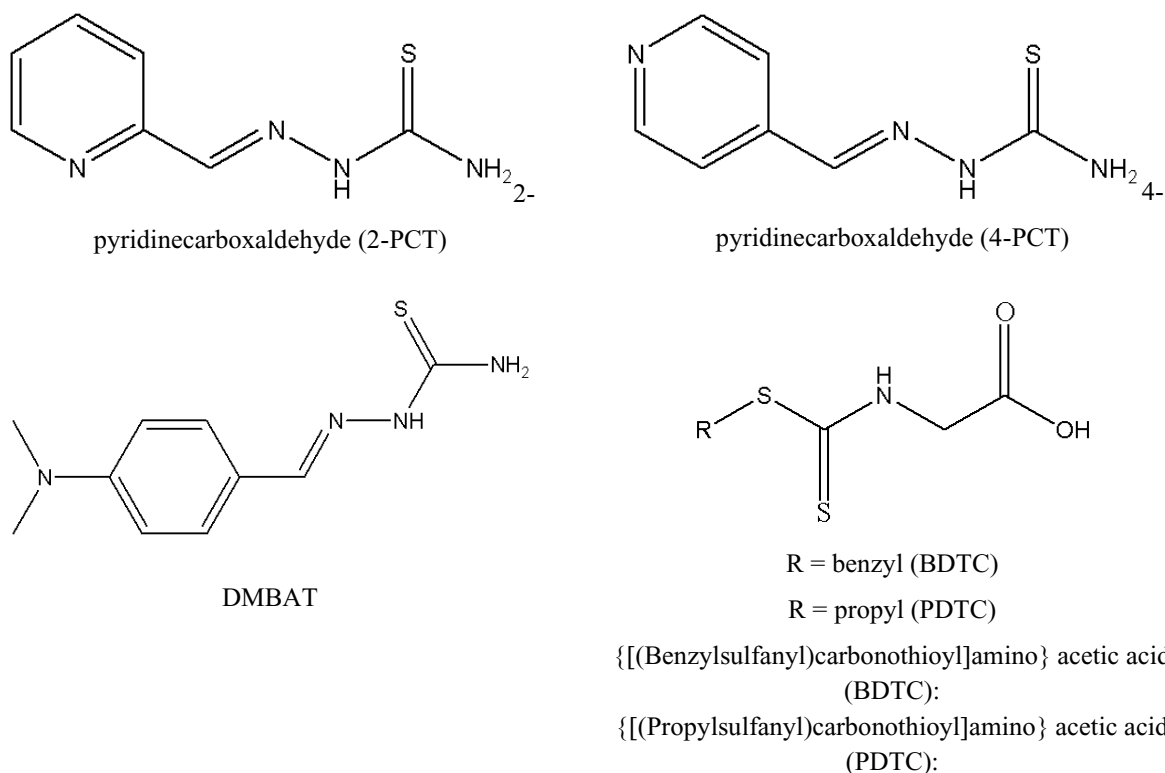


Figure 1. Structures of 2-PCT, 4-PCT, DMBAT, BDTC, and PDTC

There was a single depressed semicircle as shown in Figure 2 in all of the impedance spectra acquired for DBMAT, which consisted of two loops, one capacitive loop at a higher frequency and an inductive loop at a lower frequency. It indicated that the electrochemical solid/liquid barrier has a non-ideal capacitive behavior [20-21]. The non-homogeneity or crack (roughness) of the metal surface results in a depressed semicircle, which is attributed to frequency dispersion [22-23]. In addition, the “dispersing effect” of the depressed semicircle is a phenomenon that is commonly linked to surface roughness, chemical inhomogeneity, inhibitor adsorption, and the degree of poly crystallinity [24-26]. The existence of roughness and non-homogeneity on the metal surface because of the formation of corrosive chemicals and metal oxides might alter the density of active sites on the surface. The semicircle-shaped

Nyquist plots signify the development of a barrier on the surface and a charge transfer process that is principally responsible for metal corrosion [27]. Mourya et al. revealed that in an acid media, the DMABT [28] created a single semicircle with its center below the real axis (x-axis), indicating the existence of a single charge-transfer process during the metal dissolution [28-29]. Overall, the impedances spectra showed that the diameters of imperfect semicircles steadily increase as the inhibitor concentration rises, implying that the inhibitor molecules can prevent metal dissolution in acidic conditions and so improve corrosion resistance [18, 30]. Increased surface coverage of inhibitive molecules on the surface of metal can be linked to increased capacitive loop diameters [19, 31].

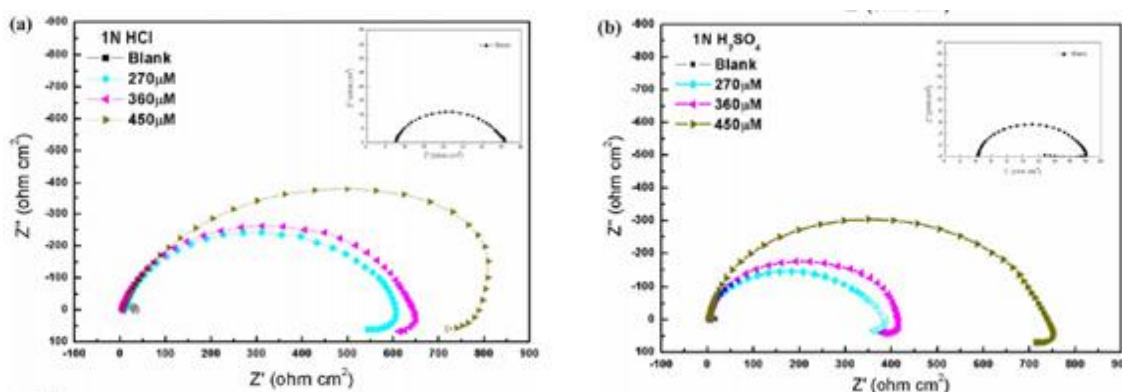


Figure 2. Nyquist plots of the corrosion of mild steel in acidic media absence and existence diverse concentrations of DMABT at 298 K: (a) 1N HCl; (b) 1N H<sub>2</sub>SO<sub>4</sub> [28]

In general, the impedance curve contains three patterns, which are the high, medium, and low frequency capacitive loops. The impedance spectra possess a large capacitive loop at high frequencies, followed by a smaller inductive loop at low frequencies. The charge transfer of the corrosion process and double-layer behavior is frequently correlated with the high-frequency capacitive loop. The relaxation process of the adsorbed intermediates regulating the anodic process could be the reason for the low inductive loop induced by the adsorption of inhibitors or  $\text{Cl}^-_{\text{ads}}$  and  $\text{H}^+_{\text{ads}}$  from HCl on the electrode surface [28, 32-33]. Additionally, the layer stabilization consequences of the corrosion action on the electrode surface, involving inhibitor molecules and their reactive products, are most likely responsible for the inductive behavior at low frequencies [32]. It could also be the outcome of passivated surface re-dissolution. The medium capacitive loop is linked to the adsorption of corrosion inhibitors on the metal surface, which increases as the inhibitor's concentration increases [32]. Mourya et al. reported that in the absence and existence of an inhibitor, the form of the curve in the two electrolytes remained unchanged [28]. This signifies that the addition of an inhibitor has no effect on the corrosion mechanism [34].

The intercept complements electrolyte resistance ( $R_s$ ), solution resistance at the higher frequency end, and electrolyte resistance ( $R_s$ ) + charge transfer resistance ( $R_{ct}$ ) at the lower frequency end. The charge transfer resistance is  $R_{ct}$ , which is the contrast between these two

quantities.  $R_{ct}$  is a measure of electron transfer over a surface that is inversely proportional to the corrosion rate [35]. Corrosion reactions that are strongly charged transfer-controlled and have impedance characteristics could be demonstrated using a simple and frequently used equivalent circuit consisting of a double layer capacitance,  $R_{ct}$ , and  $R_s$ . Instead of a pure double layer capacitance, a constant phase element, CPE, is used in the circuit compared to the capacitor, providing a more definite fit as shown in Figure 3 [36-37].

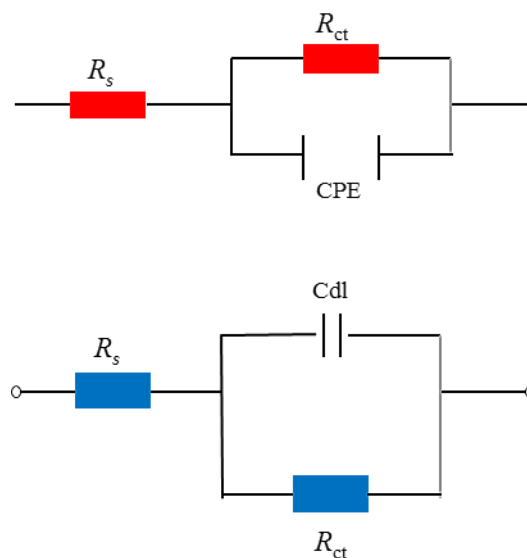


Figure 3. Equivalent circuit used to suit the EIS data of mild steel in 1N HCl consisting of diverse concentrations of inhibitors [36]

The CPE incorporates the component  $C_{dl}$  and the coefficient of exponential value of CPE  $\alpha$ , which explains physical processes such as surface roughness, inhibitor adsorption, and the development of porous layers [38-39]. A few studies reported that the  $C_{dl}$  values dropped when the concentration of various inhibitors increased and deduced that inhibitor molecules were deposited on the steel surface [36, 40-41]. In addition, lower  $C_{dl}$  values possibly be induced by a decrease in local dielectric constant and an increment in electrical double layer thickness [42-44]. The Helmholtz model can be used to explain the decreasing  $C_{dl}$  values [45]:

$$C_{dl} = \frac{\varepsilon \varepsilon_0}{\delta} S, \quad (1)$$

Where,  $\varepsilon$  = the dielectric constant of the medium,  $\varepsilon_0$  = the vacuum permittivity,  $S$  = the electrode area, and  $\delta$  = the thickness of the protective layer.

Most studies proclaimed that with the increase of inhibitor concentrations, the  $R_{ct}$  values increased. The increase in charge transfer resistance could be ascribed to the creation of a protective layer on the metal/solution interface [46-48]. The CPE's impedance function is denoted by the expression [19, 49]:

$$Z_{CPE} = Y_0^{-1} (j\omega)^{-n} \quad (2)$$

where,  $Y_0$  = a proportional factor,  $\omega$  = the angular frequency,  $n$  = a deviation parameter ( $-1 \leq n \leq +1$ );  $n$  shows phase shift that is the degree of surface inhomogeneity, and  $n = 0$ , the CPE represents a pure resistor,  $n = 1$  an inductor and for  $n = +1$ , a pure capacitor.

The values of the double layer capacitance ( $Q_{dl}$ ), and inhibition effectiveness ( $\eta$ ) are computed as follows:

$$Q_{dl} = Y_0 (\omega_m'')^{n-1} \quad (3)$$

where,  $\omega''$  = the angular frequency at the maximum value of the imaginary part of the impedance spectrum, and a constant phase angle element (CPE)  $Q_{dl}$  is used to define the  $C_{dl}$ .

According to the Helmholtz model [50], the  $Q_{dl}$  can be computed as follows:

$$Q_{dl} = \frac{\varepsilon^0 \varepsilon}{d} S \quad (4)$$

where,  $d$  = the thickness of the protective layer,  $\varepsilon^0$  is the permittivity of the air, and  $\varepsilon$  = the local dielectric constant, and  $S$  is the electrode surface area.

$$\eta = \frac{R_{ct} - R_{ct}^0}{R_{ct}} \times 100\% \quad (5)$$

$R_{ct}$  = polarization resistance values observed in the presence of the inhibitor molecule, and  $R_{ct}^0$  = polarization resistance values observed in the presence and absence of the inhibitor molecule [51].

Xu et al. reported that the values of  $R_{ct}$  rose dramatically and values of  $Q_{dl}$  decreased when the inhibitor concentration rose [19]. A reduction in  $Q_{dl}$  denotes a lowering in the local dielectric constant or a buildup in the electrical double layer thickness. As a result, the addition of 2-PCT and 4-PCT to the electrode surface may adsorb on the electrode surface by exchanging water molecules. The  $R_{ct}$  value in the blank solutions without the inhibitor is comparatively low due to the high conductivity of the HCl solution.

According to the phase angle graphs shown in Figure 1, more negative phase angle readings were observed when the concentration of corrosion inhibitors was increased in 1.0M HCl, and showed better inhibitive activity due to more inhibitor molecules adsorbed on the metal surface at higher concentrations. Adsorption of inhibitors results in increased surface smoothness [33]. Furthermore, the broadening of the curves is observed, confirming the buildup of the inhibitor molecule on the mild steel surface [52]. Nikooa et al. reported the uninhibited HCl solution exhibits a phase angle of  $-54.6^\circ$  at 63 Hz, which increases to a maximum of  $-72.6$  at 398 Hz for BDTC and  $-71.4$  at 316 Hz for PDTC [18]. It can be supported by the presence of  $\pi$  electrons in the aromatic ring of BDTC. In comparison to the PDTC, the BDTC's more planar structure provides better interaction and coverage on the metal surface.

As a conclusion from the EIS study, corrosion inhibitors are effective on metal surfaces in an acid solution, as demonstrated by the results. The inclusion of electronegativity atoms such N and S, which are active centers of adsorption, could explain the greater inhibitory effectiveness. These groups increase electron density on the adsorption centers in inhibitor compounds, enabling smoother electron transfer between the functional group and the metal. The adsorption of inhibitors on the metal surface increases

the  $R_{ct}$  because of the formation of a protective layer. Indirectly,  $Q_{dl}$  and local dielectric values decrease because of the increasing electrical double layer. An increment of surface coverage on the metal surface by corrosion inhibitors might be due to the lessening of water molecules and other ions. Besides, the impedance behavior of the metal surface was significantly altered when the inhibitor was added, and the diameter of the semicircle produced in the Nyquist plots was subsequently enlarged in the presence of inhibitors.

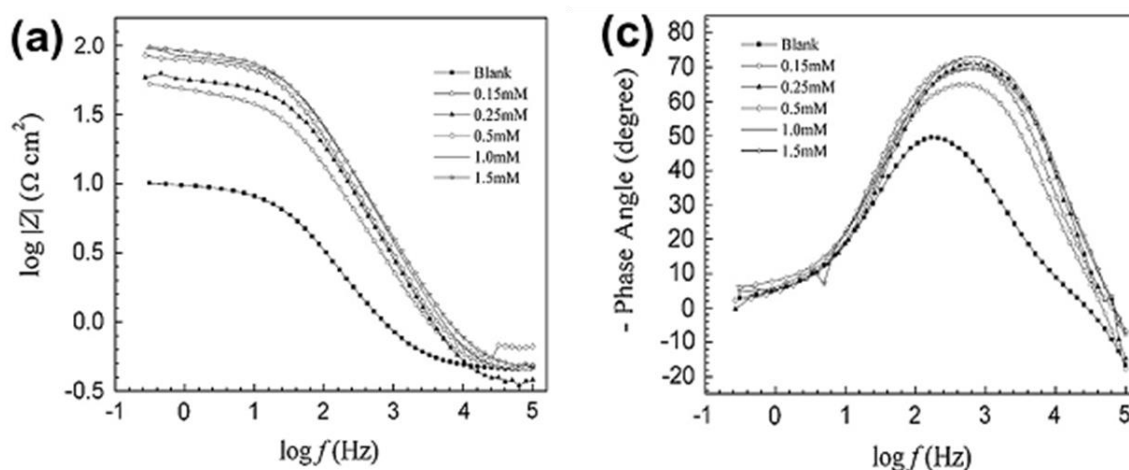


Figure 4. The Bode and Phase Angle plots for mild steel in 1.0M HCl solutions absence and existence diverse concentrations of inhibitors at 30°C: (a and c) 2-PCT [19]

### Polarization plot

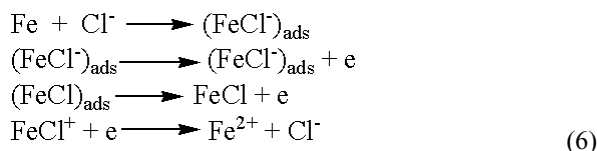
The shift in potential induced by concentration changes the environment, surrounding the electrode surface is known as concentration polarization. The voltage difference between the anode and the cathode, as well as the resistance of the corrosion cell, affects the rate of corrosion (or current density). The current flow is present in all corrosive reactions, and it changes the potential of the metal surfaces involved. Tafel curves were used to compute corrosion potentials ( $E_{corr}$ ) and corrosion current densities ( $I_{corr}$ ) [53]. The anodic reaction of corrosion occurs when metal ions from the metal surface flow into the solution or electrolyte, and the cathodic reaction occurs when hydrogen ions are discharged to form hydrogen gas or a reduction of

dissolved oxygen in acidic solutions [54]. Cao stated that if the  $E_{corr}$  of the inhibitor-containing solution is almost equivalent to the uninhibited solution, it can be deduced that the inhibition effect is mediated by adsorption inhibitive species obstructing the surface of the metal electrode geometrically [55].

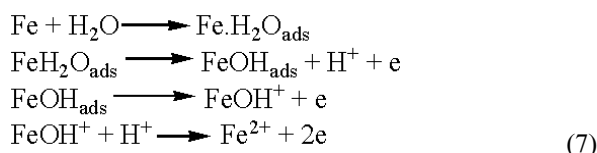
The addition of the Thiophene derivative as a corrosion inhibitor reduces the corrosion rate dramatically, lowering current densities by modifying both the anodic and cathodic Tafel curves [56]. Both anodic and cathodic reactions are impeded by this pattern, with the suppression effect becoming stronger as the inhibitor concentration rises. It is plausible that this is due to the inhibitors' adsorption at the active sites on the surface.

The mechanisms of anodic reaction in acid are shown below:

The process of Fe dissolution pathways in HCl [57]:

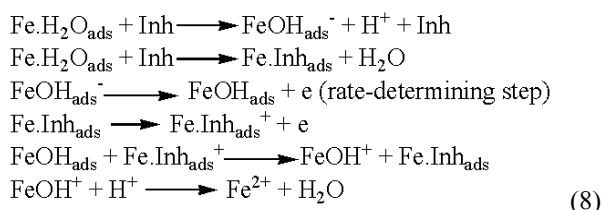


According to the mechanism depicted below, the iron electrodisolution in  $\text{H}_2\text{SO}_4$  solvent is mostly dependent on the intermediate adsorption of  $\text{FeOH}_{\text{ads}}$ :

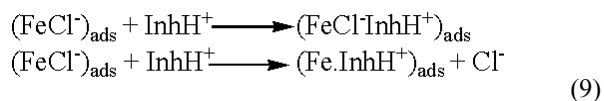


As a conclusion, Okafor and Zheng described that the anodic dissolution of iron in an  $\text{H}_2\text{SO}_4$  solution is mostly reliant on the adsorbed intermediate  $(\text{FeOH})_{\text{ads}}$ , whereas in an HCl solution, Shukla and Quraishi stated that it is mostly reliant on  $(\text{FeCl})_{\text{ads}}$  [58-59]. The corrosion inhibitors mechanism in the acid solution can be described as:

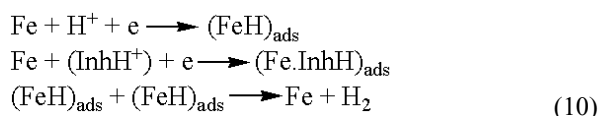
Anodic oxidation in  $\text{H}_2\text{SO}_4$  [60]:



Anodic oxidation in HCl [60]:



The adsorption of  $\text{H}^+_{\text{Inh}}$  onto the adsorbed  $\text{FeCl}^-$  present at the metal/electrolyte interface causes the  $I_{\text{corr}}$  values to drop at varied inhibitor concentrations. In the presence of corrosion inhibitor, the cathodic reaction process can be computed as follows:



The corrosion inhibitory effectiveness (Tafel) of compounds is computed using the following formula [61-62]:

$$\eta_{\text{Tafel}} (\%) = \frac{I_{\text{corr}} - I_{\text{corr(i)}}}{I_{\text{corr}}} \times 100 \quad (11)$$

where,  $i_{\text{corr}}$  = corrosion current densities in the absence of inhibitors, and  $i_{\text{corr(inh)}}$  = corrosion current densities in the absence and in the presence of inhibitors

$$\eta (\%) = \left( \frac{R_{\text{ct}} - R_{\text{ct}}^0}{R_{\text{ct}}} \right) \times 100 \quad (12)$$

where,  $R_{\text{ct}}$  = charge transfer resistance in the presence of the inhibitor, and  $R_{\text{ct}}^0$  = charge transfer resistance in the absence of the inhibitor [63].

Figure 5 shows that the  $E_{\text{corr}}$  of the corrosion inhibitors are shifted to a more negative side and the  $E_{\text{corr}}$  displacement is less than 85 mV. As a result of this finding, corrosion inhibitors were classified as mixed-type inhibitors, with cathodic polarization being the most prevalent. A reduction in the rate of anodic metal dissolution as well as a delay in the cathodic hydrogen evolution reaction reflect the inhibitors' mixed inhibitory nature [54, 68-69]. If the difference in corrosion between the inhibitor and the blank exceeded 85 mV, the inhibitor was categorized as cathodic or anodic [64-65]. As shown in Figure 6, when the inhibitors were added to the corrosive solutions, the  $E_{\text{corr}}$  values changed in a more positive manner than when they were absent. The inhibitors' corrosion potentials have shifted to the positive side and the  $E_{\text{corr}}$  displacement was less than 85 mV, indicating that they behave as mixed-type inhibitors with an anodic reaction-predominant effect. Besides, the corrosion inhibitor can be deduced by  $\beta_a$  and  $\beta_c$  values. Sahin et al. and Nazir et al. reported that  $\beta_c$  values are higher than  $\beta_a$  in different concentrations. It can be concluded that the inhibitor is predominantly cathodic in nature, as supported by the polarization curve and  $E_{\text{corr}}$  values [66-67]. The parallel cathodic current-potential curves as shown in Figure 5 implies that the addition of this inhibitor has no effect

on hydrogen evolution and that hydrogen evolution is controlled by activation. Fathabadi et al., deduced that the charge-transfer mechanism is primarily responsible for the reduction of  $H^+$  ions on the metal surface [70]. The observation can be elucidated by the fact that the metal surface has been covered with adsorbed corrosion inhibitor molecules, which has suppressed the corrosion process. This indicates that the presence of the inhibitor has no effect on the reduction pathway, and so the hydrogen evolution is retarded by the inhibitor's surface blocking effect [71-72].

The shape of polarization curves with and without the corrosion inhibitor is identical for most corrosion inhibition performance studies in the acid media. The occurrence explained that the addition of corrosion inhibitors had no impact on the corrosion mechanism of metal dissolving in acid solution, and the inhibitory impact of these inhibitors was due to the covering of inhibitor molecules at the active sites to limit their exposure to the acidic environment [73].

The inhibitor molecule attaches to the mild steel surface and blocks the anodic reaction's available reaction sites [74-75]. With increasing inhibitor concentrations, the surface coverage increases. At varying inhibitor concentrations, the surface coverage,  $\theta$  of the inhibitor was estimated using the equation:

$$\theta = \frac{i_{\text{corr}} - i_{\text{corr(inh)}}}{i_{\text{corr}}} \quad (13)$$

where;  $i_{\text{corr}}$  = corrosion current densities in the absence of inhibitors, and  $i_{\text{corr(inh)}}$  = corrosion current densities in the presence of inhibitors.

Therefore, the inhibition effectiveness can be computed using:

$$\eta(\%) = \theta \times 100 \quad (14)$$

The rise in polarization resistance in the presence of the inhibitor supports the development of a non-conducting physical barrier of compound on the metal surface, leading to an increase in corrosion inhibiting effectiveness. Besides, the formation of a plateau at anodic polarization refers to a passivation process that arises after oxygen evolution [76]. Desorption potential

is described as a sudden increase in current density with increasing potential, as evidenced by the flat region on the anodic curve. The simultaneous adsorption of inhibitor molecules on the metal surface and desorption of inhibitor molecules due to the metal's dissolution in corrosive media can explain these phenomena. The desorption rate of the inhibitor is greater than its adsorption rate in this circumstance, resulting in an increase in the corrosion current as the potential increment [77-78].

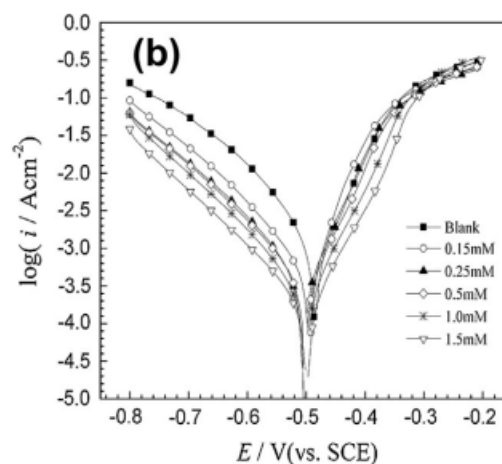


Figure 5. Potentiodynamic polarization curves for mild steel in the absence and presence of diverse concentrations of inhibitors in 1.0 M HCl: (a) 2-PCT, (b) 4-PCT at 30°C [19]

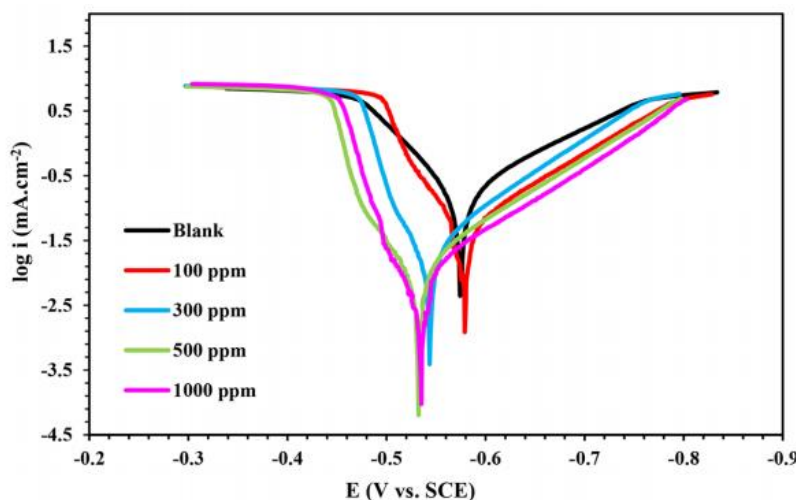


Figure 6. Potentiodynamic polarization curves for CRS in the presence and absence of diverse concentrations of the inhibitor at room temperature in 0.5 M HCl: (a) BDTC [18]

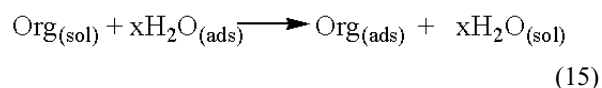
#### Scanning electron microscope-energy dispersive X-ray

SEM is used to scrutinize the morphology of mild steel surfaces before and after their immersion in acid solution. While EDX is used to confirm the creation of the protective coating owing to inhibitor adsorption on the surface of mild steel [79-80]. EDX spectra displayed the presence of N, S, P (corrosion inhibitors) and decreased composition of Fe on the metal surface as a proof of protective layer formation [81-82]. This increased inhibitory efficacy was presumably due to a strong interaction between the ( $-NH_2$ ) and ( $=S$ ) groups classified as electronegative atoms in the inhibitors' molecular structures and the metal surface, which blocks the active sites of adsorption. According to a few studies, the availability of free electron pairs, heteroatoms, and  $\pi$  orbitals permits the corrosion inhibitor to have a significant inhibitory performance, resulting in the blocking of active sites and, as a result, a reduction in corrosion rate [83]. Therefore, it improves the metal surface roughness (smoothness) and reduce the pits [84-85]. The development of iron oxide on the metal surface causes a peak of O to be extremely high in an uninhibited hydrochloride solution [86-87]. Whereas, due to the adsorption of the BDTC molecules, the oxidation of CRS on the surface is reduced, showing that there is less oxidation of CRS on the surface. The

surface of uninhibited metal is severely eroded, and due to the Cl<sup>-</sup>-induced attack, a surface deep hole can be seen at greater resolutions [88]. Besides, the corroded metal showed an uneven, pit-shaped pattern and the formation of crystal grain corrosion products [89]. Al-Amiery et al. deduced that because the surface was dried before SEM scanning, the cracks in the film are attributable to surface dehydration [90]. The electrochemical analysis correlates well with these findings.

#### Adsorption isotherm

Adsorption isotherms are commonly used to indicate the efficacy of organic adsorbent type inhibitors and are crucial in understanding how organic electrochemical reactions occur. The adsorption behavior of inhibitors can be depicted using two different types of interactions: physisorption and chemisorption. The adsorption of organic inhibitor molecules from an aqueous solution onto a metal surface has the following equilibrium equation:



From the equation, it can be deduced that the adsorption of corrosion inhibitors (organic compounds) was

complemented by the desorption of H<sub>2</sub>O molecules from the metal surface [91-92]. Langmuir, Temkin, and Frumkin isotherms, which characterizes the relationship between surface coverage,  $\theta$  and concentration of corrosion inhibitor, are the most utilized adsorption isotherms using weight loss data. Ozkir et al. surmised that an adsorption isotherm can reveal a lot about how corrosion inhibitors interact with the metal surface [93].

The following attempts were made to suit  $\theta$  values to Langmuir, Frumkin, Freundlich, and Temkin isotherms [94-96]:

$$\text{Langmuir: } \frac{C}{\theta} = \frac{1}{K} + C \quad (16)$$

$$\text{Frumkin: } \frac{\theta}{1-\theta} \exp(-2f\theta) = KC \quad (17)$$

$$\text{Temkin: } \exp(f\theta) = KC \quad (18)$$

where;  $\theta$  = surface coverage,  $K$  = the adsorption-desorption equilibrium constant or adsorptive equilibrium constant (Lmol<sup>-1</sup>),  $C$  = inhibitor concentration (molL<sup>-1</sup>), and  $f$  = factor of energetic inhomogeneity.

$$\theta = \frac{w_0 - w_i}{w_0} \quad (19)$$

$$\theta = \frac{i_{\text{corr}} - i_{\text{corr}}^{\text{inh}}}{i_{\text{corr}}} \quad (20)$$

$$\theta = \frac{R_{\text{ct}} - R_{\text{ct}}^0}{R_{\text{ct}}} \quad (21)$$

where,  $w_0$  = weight loss of metal in the blank,  $w_i$  = weight loss of metal in the inhibitor solution,  $i_{\text{corr}}$  = current density of metal in the blank,  $i_{\text{corr}}^{\text{inh}}$  = current density of metal in the inhibitor solution,  $R_{\text{ct}}$  = charge transfer resistance in the blank, and  $R_{\text{ct}}^0$  = charge transfer resistance in the inhibitor solution [36, 97, 98].

The isotherm that significantly suited the experimental data was determined using the correlation coefficient ( $R^2$ ). Mostly, the corrosion inhibition studies of organic compounds' weight losses values were fitted with Langmuir Isotherm. The Langmuir equation is based on

the presumption that the adsorption is monolayer, that all active sites have a consistent distribution of energy levels, and that adsorbed molecules do not interact with each other [99-100]. Its phenomenon is supported if the  $R^2$  value is close to 1 or unity [101]. The intercepts of the straight lines were used to compute the values of  $k_{\text{ads}}$  from the graphs of  $C/\theta$  versus  $C$  or  $\log(\theta/1-\theta)$  versus  $\log C$ . The high  $K_{\text{ads}}$  value demonstrates the inhibitor's high adsorption capacity on metal surfaces. Additionally, increasing the temperature reduced the value of  $k_{\text{ads}}$ , indicating that increasing the solution temperature generates more agitation, and consequently, the desorption of some inhibitor molecules from the metal surface [102-103]. The following equation can be applied to estimate the standard free energy of inhibitor adsorption using the value of  $k_{\text{ads}}$  [104]:

$$\Delta G_{\text{ads}}^0 = -RT \ln 55.5 k_{\text{ads}} \quad (22)$$

where, 55.5 = molar concentration of water,  $R$  = universal gas constant (8.314 JK<sup>-1</sup>mol<sup>-1</sup>),  $T$  = temperature (K), and  $\Delta G_{\text{ads}}^0$  = Gibbs free energy of adsorption.

The negative value of  $G_{\text{ads}}^0$  suggests that the process is spontaneous, implying that the inhibitor molecules are efficiently adsorbed on the mild steel surface [105]. Yurt et al. stated that the presence of electrostatic interactions between charged molecules and metal surface charges are indicated by the magnitude of  $\Delta G_{\text{ads}}^0$  smaller than 20 kJmol<sup>-1</sup> (physisorption) [106]. When  $\Delta G_{\text{ads}}^0$  is more than 40 kJmol<sup>-1</sup>, it suggests that electrons from the inhibitor molecules are shared or transferred to the metal surface, forming a coordinate type of bond (chemisorption) [107-109]. The  $\Delta G_{\text{ads}}^0$  values are in the range of -20 to -40 kJmol<sup>-1</sup>, showing that both chemisorption and physisorption are involved in the adsorption process [110-111]. Adsorption initiates electrostatic interactions between water molecules and metal surfaces, followed by chemical interactions between the metal surface and the adsorbate (inhibitor). Zhang et al. reported that if the value of  $\Delta G_{\text{ads}}^0$  is in between -20 to -40 kJmol<sup>-1</sup>, but near to -40 kJmol<sup>-1</sup>, then it can be concluded that the inhibitor is a combination of chemisorption and physisorption which is predominantly chemisorption [112]. Therefore, if the  $\Delta G_{\text{ads}}^0$  is near to -20 kJmol<sup>-1</sup>, it is predominantly physisorption.

### Conclusion

In this review paper, different techniques were discussed that will help researchers explain the phenomenon and mechanism that have occurred on the metal surface after the adsorption of the inhibitor. The type of adsorption of inhibitors on the metal surface can be deduced using electrochemical techniques (EIS and polarization), SEM-EDX, and Langmuir isotherm.

### Acknowledgement

The authors would like to thank Universiti Teknologi MARA Negeri Sembilan Branch, Kuala Pilah campus, for all the support given throughout the process of producing this paper.

### References

1. Damborenea, J. de., Conde, A. and Arenas, M. A. (2014). Chapter 3: 3 - Corrosion inhibition with rare earth metal compounds in aqueous solutions. Rare Earth-Based Corrosion Inhibitors. Woodhead Publishing Series in Metals and Surface Engineering. Elsevier.
2. Amitha, R. B. E. and Basu, B. B. J. (2012). Green inhibitors for corrosion protection of metals and alloys: an overview. *International Journal of Corrosion*, 2012: 1-15.
3. Kumar, H. and Yadav, V. (2021). Highly efficient and eco-friendly acid corrosion inhibitor for mild steel: Experimental and theoretical study. *Journal of Molecular Liquid*, 335: 1-16.
4. Danaee, I., Bahramipanah, N., Moradi, S. and Nikmanesh, S. (2016). Impedance spectroscopy studies on corrosion inhibition behavior of synthesized *n,n'*-bis(2,4-dihydroxyhydroxybenzaldehyde)-1,3-propandiimine for API-5L-X65 steel in HCl solution. *Journal of Electrochemical Science and Technology*, 7(2): 153-160.
5. Thoume, A., Elmakssoudi, A., Benmessaoud, L. D., Benzbiria, N., Benhiba, F., Dakir, M., Zahouily, M., Zarrouk, A., Azzi, M. and Zertoubi, M. (2020). Amino acid structure analog as a corrosion inhibitor of carbon steel in 0.5 M H<sub>2</sub>SO<sub>4</sub>: Electrochemical, synergistic effect and theoretical studies. *Chemical Data Collections*, 30: 1-18.
6. Dehghani, A., Mostafatabar, A. H., Bahlakeh, G., Ramezanzadeh, B. and Ramezanzadeh, M. (2020). Detailed-level computer modeling explorations complemented with comprehensive experimental studies of Quercetin as a highly effective inhibitor for acid-induced steel corrosion. *Journal of Molecular Liquid*, 309: 1-51.
7. Beytur, M., Irak, Z. T., Manap, S. and Yuksek, H. (2019). Synthesis, characterization and theoretical determination of corrosion inhibitor activities of some new 4,5-dihydro-1H-1,2,4-Triazol-5-one derivatives. *Heliyon*, 5: 1-8.
8. Ozkir, D. (2019). A newly synthesized schiff base derived from condensation reaction of 2,5-dichloroaniline and benzaldehyde: Its applicability through molecular interaction on mild steel as an acidic corrosion inhibitor by using electrochemical techniques. *Journal of Electrochemical Science and Technology*, 10(1): 37-54.
9. Marinescu, M. (2019). Recent advances in the use of benzimidazoles as corrosion inhibitors. *BMC Chemistry*, 13(136): 1-21.
10. Jamil, D. M., Al-Okbi, A. K., Al-Baghdadi, S. B., Al-Amiery, A. A., Kadhim, A., Gaaz, T. S., Kadhum, A. A. H. and Mohamad, A. B. (2018). Experimental and theoretical studies of Schiff bases as corrosion inhibitors. *Chemistry Central Journal*, 12(7): 1-9.
11. Padash, R., Rahimi-Nasrabadi, M., Rad, A. S., Sobhani-Nasab, A., Jesionowski, T. and Ehrlich, H. (2019). A theoretical study of two novel Schiff bases as inhibitors of carbon steel corrosion in acidic medium. *Applied Physic A*, 125(78): 1-11.
12. Keles, H., Emir, D. M. and Keles, M. (2015). A comparative study of the corrosion inhibition of low carbon steel in HCl solution by an imine compound and its cobalt complex. *Corrosion Science*, 101: 19-31.
13. Lgaz, H., Salghi, R., Jodeh, S. and Hammout, B. (2017). Effect of clozapine on inhibition of mild steel corrosion in 1.0 M HCl medium. *Journal of Molecular Liquid*, 225: 271-280.

14. Khaled, K. F., Samardzija, K. B. and Hackerman, N. (2006). Cobalt(III) complexes of macrocyclic-bidentate type as a new group of corrosion inhibitors for iron in perchloric acid. *Corrosion Science*, 48: 3014-3034.
15. Abdallah, M., Gad, E., Sobhi, M., Al-Fahemi, J. H. and Alfakeer, M. (2019). Performance of tramadol drug as a safe inhibitor for aluminum corrosion in 1.0M HCl solution and understanding mechanism of inhibition using DFT. *Egyptian Journal of Petroleum*, 28(2): 173-181.
16. Boughoues, Y., Benamira, M., Messaadia, L., Bouider, N. and Abdelaziz, S. (2020). Experimental and theoretical investigations of four amine derivatives as effective corrosion inhibitors for mild steel in HCl medium. *RSC Advances*, 10: 24145-24158.
17. Ferreira, E. S., Giancomelli, C., Giacomelli, F. C. and Spinelli, A. (2004). Evaluation of the inhibitor effect of L-ascorbic acid on the corrosion of mild steel. *Materials Chemistry and Physics*, 83(1): 129-134.
18. Nikoo, S. Z., Shockravi, A., Ghartavol, H. M., Halimehjani, A. Z., Ostadrahimi, M., Mirhosseini, S. M., Behzadi, H. and Ghorbani, M. (2020). A study of Glycine-based dithiocarbamates as effective corrosion inhibitors for cold rolled carbon steel in HCl solutions. *Surfaces and Interfaces*, 21: 1-67.
19. Xu, B., Yang, W., Liu, Y., Yin, X., Gong, W. and Chen, Y. (2014). Experimental and theoretical evaluation of two pyridine carboxaldehyde thiosemicarbazone compounds as corrosion inhibitors for mild steel in hydrochloric acid solution. *Corrosion Science*, 78: 260-268.
20. Mahgoub, F. M., Abdel-Nabey, B. A. and El-Samadis, Y. A. (2010). Adopting a multipurpose inhibitor to control corrosion of ferrous alloys in cooling water systems. *Materials Chemistry and Physics*, 120(1): 104-108.
21. Geoffrey, B., Dang, D. N., Stephanie, M. and Sebastien, T. (2014). Analysis of the non-ideal capacitive behaviour for high impedance organic coatings. *Progress in Organic Coatings*, 77(12): 2045-2053.
22. Aouniti, A., Elmsellema, H., Tighadouini, S., Elazzouzi, M., Radi, S., Chetouani, A., Hammouti, B. and Zarrouk, A. (2016). Schiff's base derived from 2-acetyl thiophene as corrosion inhibitor of steel in acidic medium. *Journal of Taibah University for Science*, 10: 774-785.
23. Prajila, M., Ammal, P. R. and Abraham, J. (2018). Comparative studies on the corrosion inhibition characteristics of three different triazine based Schiff's bases, HMMT, DHMMT and MHMMT. *Egyptian Journal of Petroleum*, 27(4): 467-475.
24. Chetouani, A., Medjahed, K., Benabadi, K. E., Hammouti, B., Kertit, S. and Mansri, A. (2003). Poly(4-vinylpyridine isopentyl bromide) as inhibitor for corrosion of pure iron in molar sulphuric acid. *Progress in Organic Coatings*, 46(4): 312-316.
25. Aby, P., Joby, T. K., Vinod, P. R. and Shaju, K. S. (2012). 3-Formylindole-4-aminobenzoic Acid: A potential corrosion inhibitor for mild steel and copper in hydrochloric acid media. *ISRN Corrosion*, 2012: 1-10.
26. Okonkwo, P. C., Sliem, M. H., Shakoar, R. A., Mohamed, A. M. A. and Abdullah, A. M. (2017). Effect of temperature on the corrosion behavior of API X120 pipeline steel in H<sub>2</sub>S environment. *Journal of Materials Engineering and Performance*, 26: 3775-3783.
27. Aytac, A., Ozmen, U. and Kabasakaloglu, A. (2005). Investigation of some Schiff bases as acidic corrosion of alloy AA3102. *Materials Chemistry and Physics*, 89(1): 176-181.
28. Mourya, P., Banerjee, S., Rastogi, R. B. and Singh, M. M. (2013). Inhibition of mild steel corrosion in hydrochloric and sulfuric acid media using a thiosemicarbazone derivative. *Industrial & Engineering Chemistry Research*, 52(36): 12733-12747.
29. Elias, E. E., Henry, U. N. and Damian, C. O. (2018). Synthesis and characterization of Schiff bases NBBA, MNBA and CNBA. *Heliyon*, 4(7): 1-25.

30. Jiyaul, H., Ansari, K. R., Vandana, S., Quraishi, M. A. and Obot, I. B. (2017). Pyrimidine derivatives as novel acidizing corrosion inhibitors for N80 steel useful for petroleum industry: A combined experimental and theoretical approach. *Journal of Industrial and Engineering Chemistry*, 49: 176-188.
31. Solmaz, R., Kardas, G., Çulha, M., Yazici, B. and Erbil, M. (2008). Investigation of adsorption and inhibitive effect of 2-mercaptothiazoline on corrosion of mild steel in hydrochloric acid media. *Electrochimica Acta*, 53(20): 5941-5952.
32. Khaled, K. F. (2010). Electrochemical behavior of nickel in nitric acid and its corrosion inhibition using some thiosemicarbazone derivatives. *Electrochimica Acta*, 55: 5375-5383.
33. Bhawna, C., Ashish, K. S., Sanjeeve, T., Balaram, P., Hassane, L., Ill-Min, C., Ranjana, J. and Eno, E. E. (2020). Comparative investigation of corrosion-mitigating behavior of thiadiazole-derived bis-schiff bases for mild steel in acid medium: experimental, theoretical, and surface study. *ACS Omega*, 5: 13503-13520.
34. El Basyony, N. M., Amr, E., Nady, H., Migahed, M. A. and Zaki, E. G. (2019). Adsorption characteristics and inhibition effect of two Schiff base compounds on corrosion of mild steel in 0.5 M HCl solution: experimental, DFT studies, and Monte Carlo simulation. *RSC Advances*, 9: 10473-10485.
35. Jacob, K. S. and Geetha, P. (2010). Corrosion inhibition of mild steel in hydrochloric acid solution by Schiff base furoin thiosemicarbazone. *Corrosion Science*, 52: 224-228.
36. Idouhli, R., Ousidi, A. N., Koumya, Y., Abouelfida, A., Benyaich, A., Auhmani, A. and Moulay, Y. A. I. (2018). Electrochemical studies of monoterpene thiosemicarbazones as corrosion inhibitor for steel in 1 M HCl. *International Journal of Corrosion*, 2018: 1-15.
37. Manilal, M., Sourav, K. S., Prabhas, B., Naresh, C. M., Harish, H. and Priyabrata, B. (2020). Corrosion inhibition property of azomethine functionalized triazole derivatives in 1 molL<sup>-1</sup> HCl medium for mild steel: Experimental and theoretical exploration. *Journal of Molecular Liquid*, 313: 1-15.
38. Muthukrishnan, P., Prakash, P., Jeyaprabha, B. and Shankar, K. (2019). Stigmasterol extracted from *Ficus hispida* leaves as a green inhibitor for the mild steel corrosion in 1M HCl solution. *Arabian Journal of Chemistry*, 12(8): 3345-3356.
39. Ammal, P. R., Prajila, M. and Abraham, J. (2018). Physicochemical studies on the inhibitive properties of a 1,2,4-triazole Schiff's base, HMATD, on the corrosion of mild steel in hydrochloric acid. *Egyptian Journal of Petroleum*, 27: 307-317.
40. Chitra, S., Parameswari, K. and Selvaraj, A. (2010). Dianiline Schiff bases as inhibitors of mild steel corrosion in acid media. *International Journal of Electrochemical Science*, 5: 1675-1697.
41. Ilhem, K., Tahar, D., Djamel, D., Saifi, I., Lakhdar, S. and Salah, C. (2021). Synthesis, characterization and anti-corrosion properties of two new Schiff bases derived from diamino diphenyl ether on carbon steel X48 in 1M HCl. *Journal of Adhesion Science and Technology*, 35(6): 1-31.
42. Shirin, S., Sarmin, H., Jahan, B. G., Parviz, N. and Alireza, S. (2019). Synthesis, experimental, quantum chemical and molecular dynamics study of carbon steel corrosion inhibition effect of two Schiff bases in HCl solution. *Journal of Molecular Liquid*, 285: 626-639.
43. Deng, X. and Li, X. X. (2014). Hydroxymethyl urea and 1,3-bis(hydroxymethyl) urea as corrosion inhibitors for steel in HCl solution. *Corrosion Science*, 80: 276-289.
44. Uzma, N., Zareen, A., Naveed, Z. A. and Faiz, U. S. (2019). Experimental and theoretical insights into the corrosion inhibition activity of novel Schiff bases for aluminum alloy in acidic medium. *RSC Advances*, 9: 36455-36470.
45. Khadraoui, A., Khelifa, M. H., Razika, M., Kamel, H., Tidu, A., Azari, Z., Ime, B. O. and Zarrouk, A. (2016). Extraction, characterization and anti-corrosion activity of *Mentha pulegium* oil: Weight loss, electrochemical, thermodynamic and surface studies. *Journal of Molecular Liquid*, 216: 724-731.

46. Nimmy, K., Joby, T. K., Vinod, P. R. and Shaju, K. S. (2014). Electrochemical impedance spectroscopy and potentiodynamic polarization analysis on anticorrosive activity of thiophene-2-carbaldehyde derivative in acid medium. *Indian Journal of Materials Science*, 2014: 1-6.
47. Hamdani, N. E., Fdil, R., Tourabi, M., Jama, C. and Bentiss, F. (2015). Alkaloids extract of *Retama monosperma* (L.) Boiss. seeds used as novel eco-friendly inhibitor for carbon steel corrosion in 1 M HCl solution: Electrochemical and surface studies. *Applied Surface Science*, 357: 1294-1305.
48. Turuvekere, K. C., Kikkeri, N. S. M. and Harmesh, C. T. (2015). Thermodynamic, electrochemical and quantum chemical evaluation of some triazole Schiff bases as mild steel corrosion inhibitors in acid media. *Journal of Molecular Liquid*, 211: 1026-1038.
49. Ragi, K., Joby, T. K., Vinod, P. R., Sini, V. C. and Binsi, M. P. (2019). Synthesis, cyclic voltammetric, electrochemical, and gravimetric corrosion inhibition investigations of schiff base derived from 5,5-dimethyl-1,3-cyclohexanedione and 2-aminophenol on mild steel in 1 M HCl and 0.5 M H<sub>2</sub>SO<sub>4</sub>. *International Journal of Electrochemistry*, 2019: 1-13.
50. Weihua, L., Qiao, H., Changling, P. and Baorong, H. (2007). Experimental and theoretical investigation of the adsorption behaviour of new triazole derivatives as inhibitors for mild steel corrosion in acid media. *Electrochimica Acta*, 52(22): 6386-6394.
51. Ifzan, A., Aamer, S., Pervaiz, A. C., Syeda, A. S., Muhammad, N. A. and Muhammad, S. (2020). Bis-Schiff bases of 2,2'-dibromobenzidine as efficient corrosion inhibitors for mild steel in acidic medium. *RSC Advances*, 10: 4499-4511.
52. Yadav, M., Kumar, S., Sinha, R. R. and Kumar, S. (2014). Experimental and theoretical studies on synthesized compounds as corrosion inhibitor for mild steel in hydrochloric acid solution. *Journal of Dispersion Science and Technology*, 35: 1751-1763.
53. Poorqasemi, E., Abootalebi, O., Peikari, M. and Haqdar, F. (2009). Investigating accuracy of the Tafel extrapolation method in HCl solutions. *Corrosion Science*, 51: 1043-1054.
54. Sam, J., Jeevana, R., Aravindakshan, K. K. and Abraham, J. (2017). Corrosion inhibition of mild steel by *n*(4)-substituted thiosemicarbazone in hydrochloric acid media. *Egyptian Journal of Petroleum*, 26: 405-412.
55. Cao, C. (1996). On electrochemical techniques for interface inhibitor research. *Corrosion Science*, 38 (12): 2073-2082.
56. Zachariah, P. M., Keerthi, R., Cyril, A., Bincy, J. and Sam, J. (2020). Corrosion inhibition of mild steel using poly (2-ethyl -2-oxazoline) in 0.1M HCl solution. *Heliyon*, 6(11): 1-8.
57. Poornima, T., Nayak, J. and Shetty, A. N. (2012). Effect of diacetyl monoxime thiosemicarbazone on the corrosion of aged 18 Ni 250 grade maraging steel in sulphuric acid solution. *Journal of Metallurgy*, 2012: 1-13.
58. Okafor, P. C. and Zheng, Y. (2009). Synergistic inhibition behaviour of methylbenzyl quaternary imidazoline derivative and iodide ions on mild steel in H<sub>2</sub>SO<sub>4</sub> solutions. *Corrosion Science*, 51: 850-859.
59. Shukla, S. K. and Quraishi, M. A. (2010). The effects of pharmaceutically active compound doxycycline on the corrosion of mild steel in hydrochloric acid solution. *Corrosion Science*, 52: 314-321.
60. Okafor, P. C., Ikpi, M. E., Uwah, I. E., Ebenso, E. E., Ekpe, U. J. and Umoren, S. A. (2008). Inhibitory action of *Phyllanthus amarus* extracts on the corrosion of mild steel in acidic media. *Corrosion Science*, 50 (8): 2310-2317.
61. Kassim, K., Kamal, N. K. M. and Fadzil, A. H. (2016). Synthesis, characterization and electrochemical studies of 4-methoxybenzoylthiourea derivatives. *Malaysian Journal of Analytical Sciences*, 20(6): 1311-1317.
62. Verma, C., Olasunkanmi, L. O., Obot, I. O., Ebenso, E. E. and Quraishi, M. A. (2016). 5-Arylpyrimido-[4,5-b] quinoline-diones as new and sustainable corrosion inhibitors for mild steel in 1 M HCl: a combined experimental and theoretical approach. *RSC Advances*, 6(19): 15639-15654.

63. Sourav, K. S., Alok Dut, D., Pritam, G., Dipankar, S. and Priyabrata, B. (2016). Novel Schiff-base molecules as efficient corrosion inhibitors for mild steel surface in 1 M HCl medium: experimental and theoretical approach. *Physical Chemistry Chemical Physics*, 18(27): 17898-17911.
64. Fouda, A. S., El-Desoky, H. S., Abdel-Galeil, M. A. and Dina, M. (2021). Niclosamide and dichlorophenamide: new and effective corrosion inhibitors for carbon steel in 1M HCl solution. *SN Applied Sciences*, 3(287): 1-20.
65. Ghulamullah, K., Wan, J. B., Salim, N. K., Pervaiz, A., Ladan, M., Ahmed, S. M., Khan, G. M., Rehman, M. A. and Mohamad Badry, A. B. (2017). Electrochemical investigation on the corrosion inhibition of mild steel by Quinazoline Schiff base compounds in hydrochloric acid solution. *Journal of Colloid and Interface Science*, 502: 134-145.
66. Sahin, M., Bilgic, S. and Yilmaz, H. (2002). The inhibition effects of some cyclic nitrogen compounds on the corrosion of the steel in NaCl mediums. *Applied Surface Science*, 195(1-4): 1-7.
67. Nazir, U., Akhter, Z., Janjua, N. K., Asghar, M. A., Kanwal, S., Butt, T. M., Sani, A., Liaqat, F., Hussain, R. and Shah, F. U. (2020). Biferrocenyl Schiff bases as efficient corrosion inhibitors for an aluminium alloy in HCl solution: a combined experimental and theoretical study. *RSC Advances*, 10: 7585-7599.
68. Prabakaran, M., Kim, S. H., Hemapriya, V., Gopiraman, M., Kim, I. S. and Chung, I. M. (2016). Rhus verniciflua as a green corrosion inhibitor for mild steel in 1 M H<sub>2</sub>SO<sub>4</sub>. *RSC Advances*, 6(62): 57144-57153.
69. Goulart, C. M., Esteves-Souza, A., Martinez-Huitle, C. A., Rodrigues, C. J. F., Maciel, M. A. M. and Echevarria, A. (2013). Experimental and theoretical evaluation of semicarbazones and thiosemicarbazones as organic corrosion inhibitors. *Corrosion Science*, 67: 281-291.
70. Fathabadi, H. E., Ghorbani, M. and Ghartavol, H. M. (2021). Corrosion inhibition of mild steel with tolyltriazole. *Materials Research*, 24(4): 1-16.
71. Ehteshamzadeh, M., Jafari, A. H., Naderi, E. and Hosseini, M. G. (2009). Effect of carbon steel microstructures and molecular structure of two new Schiff base compounds on inhibition performance in 1 M HCl solution by EIS. *Materials Chemistry and Physics*, 113(2-3): 986-993.
72. Govindaraju, K. M., Gopi, D. and Kavitha, L. (2009). Inhibiting effects of 4-amino-antipyrine based schiff base derivatives on the corrosion of mild steel in hydrochloric acid. *Journal of Applied Electrochemistry*, 39: 2345-2352.
73. Satapathy, A. K., Gunasekaran, G., Sahoo, S. C., Amit, K. and Rodrigues, P. V. (2009). Corrosion inhibition by *Justicia gendarussa* plant extract in hydrochloric acid solution. *Corrosion Science*, 51(12): 2848-2856.
74. Ebenso, E. E., Arslan, T., Kandemirli, F., Caner, N. and Love, I. (2010). Quantum chemical studies of some rhodanine azosulpha drugs as corrosion inhibitors for mild steel in acidic medium. *International Journal of Quantum Chemistry*, 110(5): 1003-1018.
75. Solmaz, R. (2010). Investigation of the inhibition effect of 5-((E)-4-phenylbuta-1,3-dienylideneamino)-1,3,4-thiadiazole-2-thiol Schiff base on mild steel corrosion in hydrochloric acid. *Corrosion Science*, 52 (10): 3321-3330.
76. Masahiko, T., Kazushige, I., Yoichi, W., Motohiro, A. and Motomasa, F. (2009). Study of polarization curve measurement method for type 304 stainless steel in BWR high temperature-high purity water. *Journal of Nuclear Science and Technology*, 46(2): 132-141.
77. Chakravarthy, M. P., Mohana, K. N. and Pradeep Kumar, C. B. (2014). Behaviour of nicotinamide derivatives on mild steel in hydrochloric acid solution. *International Journal of Industrial Chemistry*, 5 (19): 1-21.
78. Lorenz, W. J. and Mansfeld, F. (1982). Determination of corrosion rates by electrochemical DC and AC methods. *Corrosion Science*, 21(9-10): 647-672.
79. Youcef, B., Fatiha, B. and Saida, K. (2021). A new corrosion inhibitor for steel rebar in concrete: Synthesis, electrochemical and theoretical studies. *Journal of Molecular Structure*, 1225: 1-17.

80. Abdelghani, M., Lakhdar, S., Abdelkader, H., Ilhem, K. and Embarek, B. (2021). Synthesis, density functional theory study, molecular dynamics simulation and anti-corrosion performance of two benzidine Schiff bases. *Journal of Molecular Structure*, 1235: 1-15.
81. Merah, S., Larabi, L., Abderrahim, O. and Harek, Y. (2017). Study of corrosion inhibition of C38 steel in 1 M HCl solution by polyethyleneiminemethylene phosphonic acid. *International Journal of Industrial Chemistry*, 8: 263-272.
82. Xifeng, Y., Feng, L. and Weiwei, Z. (2019). 4-(Pyridin-4-yl) thiazol-2-amine as an efficient non-toxic inhibitor for mild steel in hydrochloric acid solutions. *RSC Advances*, 9: 10454-10464.
83. Laabaissi, T., Benhiba, F., Missioui, M., Rouifi, Z., Rbaa, M., Oudda, H., Ramli, Y., Guenbour, A., Warad, I. and Zarrouk, A. (2020). Coupling of chemical, electrochemical and theoretical approach to study the corrosion inhibition of mild steel by new quinoxaline compounds in 1 M HCl. *Heliyon*, 6(5): 1-15.
84. Quy, H. D., Tran, D. and Nam, P. C. (2021). A Study of 1-benzyl-3-phenyl-2-thiourea as an effective steel corrosion inhibitor in 1.0 M HCl Solution. *Journal of Chemistry*, 2021: 1-14.
85. Parul, D., Quraishi, M. A. and Obot, I. B. (2018). A combined electrochemical and theoretical study of pyridine-based Schiff bases as novel corrosion inhibitors for mild steel in hydrochloric acid medium. *Journal of Chemical Sciences*, 130(8): 1-19.
86. Kumari, P. P., Shetty, P. and Rao, S. A. (2017). Electrochemical measurements for the corrosion inhibition of mild steel in 1 M hydrochloric acid by using an aromatic hydrazide derivative. *Arabian Journal of Chemistry*, 10(5): 653-663.
87. Maryam, C., Abdelkarim, C., Hassane, L., Rachid, S., Santosh, L. G., Bhat, K. S., Riadh, M., Ismat, H. A., Mohammad, I. K., Hiroki, S. and Ill-Min, C. (2020). Synthesis and corrosion inhibition evaluation of a new schiff base hydrazone for mild steel corrosion in HCl medium: electrochemical, DFT, and molecular dynamics simulations studies. *Journal of Adhesion Science and Technology*, 34(12): 1283-1314.
88. Zhenzhen, Z., Min, S., Yiming, J., Li, L. and Jin, L. (2016). Effect of tin on the corrosion resistance of 16 Cr ferritic stainless steel in acidic solution and chloride-containing media. *International Journal of Electrochemical Science*, 11: 3963-3975.
89. Zesheng, C., Zheng, L., Kun-Huan, H., Guo-Cheng, H., Yiju, L., Jiaying, H. and Xianmei, W. (2021). Two diamine Schiff base as a corrosion inhibitor for carbon steel in sulfuric acid solution: Electrochemical assessment and theoretical calculation. *International Journal of Electrochemical Science*, 16: 1-21.
90. Al-Amiery, A. A., Kassim, F. A., Kadhum, A. A. H. and Mohamad, A. B. (2016). Synthesis and characterization of a novel eco-friendly corrosion inhibition for mild steel in 1 M hydrochloric acid. *Scientific Reports*, 6: 1-13.
91. Negm, N. A., Kandile, N. G., Badr, E. A. and Mohammed, M. A. (2012). Gravimetric and electrochemical evaluation of environmentally friendly nonionic corrosion inhibitors for carbon steel in 1 M HCl. *Corrosion Science*, 65: 94-103.
92. Narvaez, L., Cano, E. and Bastidas, D. M. (2005). 3-Hydroxybenzoic acid as AISI 316L stainless steel corrosion inhibitor in a H<sub>2</sub>SO<sub>4</sub>-HF-H<sub>2</sub>O<sub>2</sub> pickling solution. *Journal of Applied Electrochemistry*, 35: 499-506.
93. Ozkır, D., Kayakırlmaz, K., Bayol, E., Gürten, A. A. and Kandemirli, F. (2012). The inhibition effect of Azure A on mild steel in 1 M HCl. A complete study: Adsorption, temperature, duration and quantum chemical aspects. *Corrosion Science*, 56: 143-152.
94. Agrawal, R. and Namboodhiri, T. K. G. (1990). The inhibition of sulphuric acid corrosion of 410 stainless steel by thioureas. *Corrosion Science*, 30(1): 37-52.
95. Zhao, T. P. and Mu, G. N. (1999). The adsorption and corrosion inhibition of anion surfactants on aluminium surface in hydrochloric acid. *Corrosion Science*, 41: 1937-1944.

96. Yaro, A. S., Khadom, A. A. and Ibraheem, H. F. (2011). Peach juice as an anticorrosion inhibitor of mild steel. *Anti-Corrosion Methods and Materials*, 58(3): 116-124.
97. Hegazy, M. A., Hasan, A. M., Emara, M. M., Bakr, M. F. and Youssef, A. H. (2012). Evaluating four synthesized Schiff bases as corrosion inhibitors on the carbon steel in 1 M hydrochloric acid. *Corrosion Science*, 65: 67-76.
98. Goulart, C. M., Esteves-Souza, A., Martinez-Huitle, C. A., Rodrigues, C. J. F., Maciel, M. A. M. and Echevarria, A. (2013). Experimental and theoretical evaluation of semicarbazones and thiosemicarbazones as organic corrosion inhibitors. *Corrosion Science*, 67 (3): 281-291.
99. Muthukrishnan, P., Jeyaprabha, B. and Prakash, P. (2017). Adsorption and corrosion inhibiting behavior of *Lannea coromandelica* leaf extract on mild steel corrosion. *Arabian Journal of Chemistry*, 10: 2343-2354.
100. Adewuyi, A., Gopfert, A. and Wolf, T. (2014). Succinyl amide gemini surfactant from *Adenopus breviflorus* seed oil: A potential corrosion inhibitor of mild steel in acidic medium. *Industrial Crops and Products*, 52: 439-449.
101. Ji, G., Shukla, S. K., Dwivedi, P., Sundaram, S. and Ebenso, E. E. (2012). Green *Capsicum annum* fruit extract for inhibition of mild steel corrosion in hydrochloric acid solution. *International Journal of Electrochemical Science*, 7: 12146-12158.
102. Gopiraman, M., Selvakumaran, N., Kesavan, D. and Karvembu, R. (2012). Adsorption and corrosion inhibition behaviour of N-(phenylcarbamothioyl) benzamide on mild steel in acidic medium. *Progress in Organic Coatings*, 73 (1): 104-111.
103. Ahamad, I., Prasad, R. and Quraishi, M. A. (2010). Inhibition of mild steel corrosion in acid solution by Pheniramine drug: experimental and theoretical study. *Corrosion Science*, 52 (9): 3033-3041.
104. Fazayel, A. S., Khorasani, M. and Sarabi, A. A. (2018). The effect of functionalized polycarboxylate structures as corrosion inhibitors in a simulated concrete pore solution. *Applied Surface Science*, 441: 895-913.
105. Singh, A. K. and Quraishi, M. A. (2010). Inhibiting Effects of 5-Substituted Isatin-Based Mannich Bases on the Corrosion of Mild Steel in Hydrochloric Acid Solution. *Journal of Applied Electrochemistry*, 40 (7): 1293-1306.
106. Yurt, A., Bereket, G., Kivrak, A., Balaban, A. and Erk, B. (2005). Effect of Schiff bases containing pyridyl group as corrosion inhibitors for low carbon steel in 0.1 M HCl. *Journal of Applied Electrochemistry*, 35: 1025-1032.
107. Saliyan, V. R. and Adhikari, A. V. (2008). Quinolin-5-ylmethylene-3-{[8-(trifluoromethyl)quinolin-4-yl] thio}propanohydrazide as an effective inhibitor of mild steel corrosion in HCl solution. *Corrosion Science*, 50 (1): 55-61.
108. Deyab, M. A. (2015). Egyptian licorice extract as a green corrosion inhibitor for copper in hydrochloric acid solution. *Journal of Industrial and Engineering Chemistry*, 22: 384-389.
109. Abd El-Lateef, H. M., Abu-Dief, A. M., Abdel-Rahman, L. H., Sanudo, E. C. and Aliaga-Alcalde, N. (2015). Electrochemical and theoretical quantum approaches on the inhibition of C1018 carbon steel corrosion in acidic medium containing chloride using some newly synthesized phenolic Schiff bases compounds. *Journal of Electroanalytical Chemistry*, 743: 120-133.
110. Sigircik, G., Tuken, T. and Erbil, M. (2015). Inhibition effectiveness of aminobenzonitrile compounds on steel surface. *Applied Surface Science*, 324: 232-239.
111. Kowsari, E., Payami, M., Amini, R., Ramezanzadeh, B. and Javanbakht, M. (2014). Task-specific ionic liquid as a new green inhibitor of mild steel corrosion. *Applied Surface Science*, 289: 478-486.
112. Zhang, H. H., Qin, C. K., Chen, Y. and Zhang, Z. (2019). Inhibition behaviour of mild steel by three new benzaldehyde thiosemicarbazone derivatives in 0.5 M H<sub>2</sub>SO<sub>4</sub>: Experimental and computational study. *Royal Society Open Science*, 6(8): 1-19.